ACTA CHEMICA SCANDINAVICA 19 (1965) 1955–1968

Studies on the Failure of the First Born Approximation in Electron Diffraction

I. Uranium Hexafluoride

HANS M. SEIP

Department of Chemistry, University of Oslo, Blindern, Oslo 3, Norway

The structure of uranium hexafluoride has been studied by electron diffraction. There is no evidence for deviation from O_h symmetry. The U–F bond length is 1.999 Å with a standard deviation of 0.003 Å. The root-mean-square amplitudes of vibration are the same as found from spectroscopic data within the experimental error limits. Scattering amplitudes calculated by different authors, have been used. It is demonstrated that the theoretical values fit the experimental data reasonably well.

THEORY

The scattering of electrons by a central force field is treated in many textbooks of quantum mechanics.[1,3] Some aspects of the scattering theory have also been treated in two recent review articles.[4,5] The classical treatment of the scattering process leads to a real scattering amplitude which for an atom is proportional to $[Z - F(s)]/s^2$ where Z is the atomic number and $F(s)$ the scattering factor. The quantum mechanical treatment yields a complex scattering amplitude. The result may be written as

$$f(\vartheta) = \sum_{l=0}^{\infty} (2\ l + 1)\ [\{\exp(2i\delta_l) - 1\}/2ik]\ P_l(\cos\vartheta) \qquad (1)$$

P_l is the Legendre polynomial of order l.

$$k^2 = \frac{8\pi^2 m}{h^2} E$$

δ_l is the phase shift of the l'th partial wave. These phase shifts can be determined by solving the appropriate Schrödinger equation. The theoretical molecular intensity expression is somewhat different according to the theory used. Eqn. (2) gives the formula found by the classical treatment.

$$I_m^{c.}(s) = \text{const}\frac{1}{s}\sum_{i\neq j}\sum \frac{(Z_i - F_i)}{s^2}\ \frac{(Z_j - F_j)}{s^2} \exp(-\tfrac{1}{2}u_{ij}^2 s^2)[(\sin r_{ij}s)/r_{ij}] \qquad (2)$$

If we put

$$f(s) = |f(s)| \exp[i\eta(s)] \tag{3}$$

the corresponding quantum mechanical expression is

$$I_m^{q.m.}(s) = \text{const} \frac{1}{s} \sum_{i \neq j} \sum |f_i| |f_j| \cos(\eta_i(s) - \eta_j(s)) \exp(-\tfrac{1}{2} u_{ij}^2 s^2) [(\sin r_{ij} s)/r_{ij}] \tag{4}$$

It is convenient to define an intensity function by

$$I(s) = s^5 I_m^c(s) / (Z_k - F_k)(Z_l - F_l) \tag{5}$$

if the classical $I_m(s)$ function (2) is used, and by

$$I(s) = s I_m^{q.m.}(s) / |f_k||f_l| \tag{6}$$

if $I_m(s)$ is given by eqn. (4).
Thus we get

$$I(s) = \text{const} \sum_{i \neq j} \sum g_{ij}(s) \exp(-\tfrac{1}{2} u_{ij}^2 s^2) [(\sin r_{ij} s)/r_{ij}] \tag{7}$$

where

$$g_{ij}(s) = \frac{(Z_i - F_i)(Z_j - F_j)}{(Z_k - F_k)(Z_l - F_l)} \tag{8}$$

in the classical theory, and

$$g_{ij}(s) = \frac{|f_i| \; |f_j|}{|f_k| \; |f_l|} \cos(\Delta\eta_{ij}) \tag{9}$$

in the quantum mechanical theory.

Experience shows that the classical $g_{ij}(s)$ expression (8) may be used when molecules with only light atoms are studied if the electron velocity is sufficiently high.

The expression (8) may in many cases be approximated by a constant. If this is the case for all the $g_{ij}(s)$ functions, it follows from (7) that the intensity is a sum of damped sine curves. The fraction in eqn. (9) (containing the $|f|$ values) is usually not too different from the classical expression. (8). The difference is considerable only if some of the atoms are very heavy. The effect of the cosine factor in eqn. (9) depends mainly on the difference $|Z_i - Z_j|$, though the actual atomic numbers and the value of u_{ij} are also of importance. $\cos(\Delta\eta_{ij})$ is close to unity for very small differences in the atomic numbers and may usually be neglected if the difference is less than 5. For somewhat greater values of $|Z_i - Z_j|$ (say 5—15) the cosine factor will operate as an additional damping, since a cosine function may be approximated by an exponential function for small values of the argument. One may therefore often neglect the cosine factor in the intensity expression if the proper corrections are made to the u values. If $|Z_i - Z_j|$ is larger than 15, the use of eqn. (9) in the intensity expression is recommended.

The theoretical intensity expression (7) holds true only if each pair of atoms may be considered as an independet harmonic oscillator. An approximate

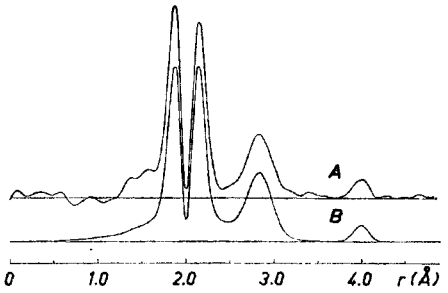

Fig. 1. Experimental (A) and theoretical (B) RD curves. $k = 0.002$ Å^2.

formula for the intensity function in the case of anharmonic vibrations, has been given by Bartell [6,7] as

$$I(s) = \text{const} \sum_{i \neq j} g_{ij}(s) \exp(-\tfrac{1}{2}u_{ij}^2 s^2) \frac{\sin[(r_{ij} - \varkappa_{ij} s^2)s]}{r_{ij}} \quad (10)$$

$\varkappa_{ij}$ is a constant determined by the anharmonicity.*

A radial distribution (RD) function is defined by

$$\sigma(r)/r = \int I(s) \exp(-ks^2) \sin(rs)\, ds \quad (11)$$

where k is an artificial damping constant.

Distances for which eqn. (7) may be used with the approximation g_{ij} = constant, are represented by Gaussian peaks in the RD curve. The experimental RD curve for UF_6 is shown in Fig. 1 (curve A). The two outer peaks represent the F...F distances while the two inner peaks are the U—F contribution. A structure with two different U—F bond lenghts was therefore originally proposed. [8,9] However, spectroscopic measurements strongly indicated O_h symmetry.[10] This discrepancy was first explained by Glauber and Schomaker.[11,12] They showed that if the proper formula (9) is used, the RD curve will have two peaks for a single U—F bond length.

Complex scattering amplitudes have been calculated by Ibers and Hoerni [13] and by Karle and Bonham.[14,15] The phase shifts (δ_l in eqn. (1)) were calculated in the WKB approximation by Ibers and Hoerni assuming Thomas-Fermi potentials in most of the calculations. The WKB method was also used by Karle and Bonham, but they have carried out numerical integration of the radial Schrödinger equation as well. Hartree-Fock potentials were assumed for light atoms and Thomas-Fermi-Dirac potentials in other cases. It is difficult to estimate the accuracy of these calculations. We have therefore investigated some molecules where the classical theory definitely fails, to see if satisfactory agreement between theoretical and experimental intensity curves and RD curves is obtained when the quantum mechanical formulas are used.

UF_6 is well suited for this investigation since the difference in the atomic numbers is very large (92—9 = 83). The compound has been studied before, but intensity values were not obtained to very high s values.[12,16,17]

* The term anharmonicity is rather unfortunate, but commonly used in this connection. One might rather say that $\varkappa_{ij}$ is determined by the deviation from symmetry in the distance distribution.

EXPERIMENTAL

The sample of uranium hexafluoride was obtained from Baker and Adamson, New York. Diffraction photographs were taken in the usual way at a nozzle temperature of about 70°C. The accelerating potential was approximately 35 kV. Three camera distances were used (48.13 cm, 23.36 cm and 12.53 cm) giving intensity data in the three ranges

$s = 1.25 - 20.25$ Å^{-1}, $s = 2.50 - 40.00$ Å^{-1}, $s = 14.50 - 63.00$ Å^{-1}.

Four plates were selected at each distance. The plates were photometered, and the data corrected in a manner described elsewhere.[5,18] An experimental background was subtracted from the total intensity.

STRUCTURE ANALYSIS

In this case it seemed reasonable to multiply the molecular intensity by $s/|f_F|^2$ (*cf.* eqn. (6)). The contribution from the F...F distances to the total intensity function is then simply two damped sine curves in the harmonic approximation. These distances are represented by Gaussian peaks in the theoretical radial distribution curve (Fig. 1). The F...F contribution is relatively small compared to the U—F contribution.

Fig. 2 shows the experimetal intensity function (curve A). Two theoretical intensity functions, both based upon a regular octahedral model, were calculated according to eqn. (7), but with different g_{ij} functions. The r- and u values used in these calculations are given in Table 2 a. They were obtained by refinements described in the following section. Curve B was obtained by using eqn. (9) and scattering amplitudes calculated according to the method described by Karle and Bonham.[15*] Cos $(\eta_U - \eta_F)$ is equal to zero near $s = 10$ Å^{-1} $(\eta_U - \eta_F = \pi/2)$ and $s = 51$ Å^{-1} $(\eta_U - \eta_F = 3\pi/2)$. The intensity must accordingly be very small near these s values. Intensity data were, as mentioned, recorded to $s = 63$ Å^{-1}. However, the curves in Fig. 2 are plotted only to $s = 44.25$ Å^{-1}. The rest of the data was neglected because of noise. Unfortunately the noise made it difficult to identify a growing U—F intensity beyond $s = 51$ Å^{-1}. Curve C in Fig. 2 corresponds to the classical theory. Eqn. (8) was used and the scattering factors were calculated by Hanson *et al.*[19]

An experimental RD curve is given in Fig. 1 (A). The damping constant $k = 0.002$ Å^2. Approximate values for the interatomic distances may be found directly from this curve. The position of the maxima (or the center of gravity) of the two outer peaks gives the F... F distances, while the U—F distance is taken at the minimum between the two peaks. The u values for the F... F distances are also readily found from the half-widths of the corresponding peaks. The u value for the U—F bond may be determined by comparing the experimental curve with a series of theoretical ones with different u values. The theoretical RD curve given (curve B in Fig. 1) is found by a Fourier transformation of the theoretical intensity curve (B) in Fig. 2. Thus the distances and u values are those given in Table 2 a.

* The f values were calculated for the applied electron velocity by T. Strand on computer programs written by R. A. Bonham. δ_l was determined by the WKB method for $l = 0 - 24$ and by Born's phase shift formula for $l = 25 - 124$.

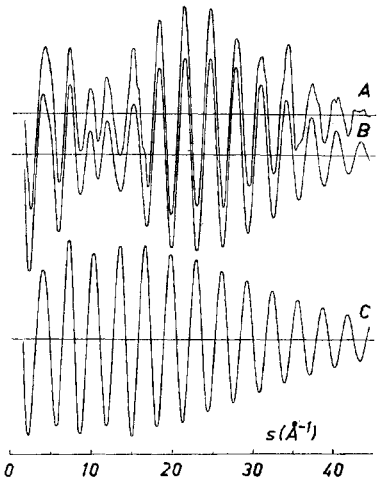

Fig. 2. Experimental (A) and theoretical intensity curves. The theoretical curves were calculated according to eqn. (7) with the r and u values given in Table 2 a. Curve B was obtained using eqn. (9) with scattering amplitudes from Karle and Bonham.[15] Curve C was obtained using eqn. (8) and scattering factors from Hanson *et al.*[19]

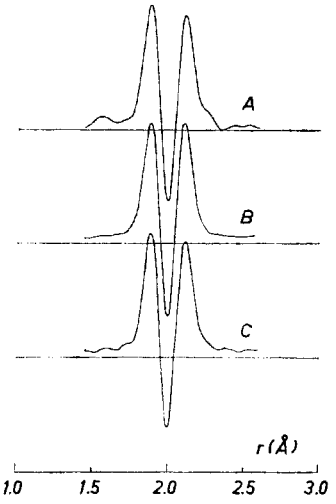

Fig. 3. The U—F double peak in RD curves calculated with $k = 0$ Å^3. A is the experimental curve. B is the theoretical curve based on harmonic vibrations. C is the theoretical curve based on anharmonic vibrations.

The minimum corresponding to the U—F distance is deeper if a smaller damping constant is used. Fig. 3 curve A shows the experimental double peak when $k = 0$ Å^2. Curve B is the theoretical curve calculated as before, but with zero damping. The curves A and B are quite similar. However, one difference is observed: While the inner peak is higher than the outer one in the experimental curve, the heights are equal in curve B. Since curve B was obtained by a Fourier transformation of an intensity function calculated according to eqn. (7), it is based on the assumption of harmonic vibrations. A theoretical intensity function was then calculated according to expression (10) (including anharmonicity) with the parameters given in Table 2 e. When this intensity function was Fourier transformed, curve C in Fig. 3 was obtained. The ratio of the heights of the two peaks is 0.916 in this curve compared to 0.919 in the experimental curve (A). However, the value used for $\varkappa_{UF}$ is rather large (see page 1962).

LEAST-SQUARES REFINEMENT

As mentioned the distances and u values may be found directly from the RD curve, but these parameters may also be determined by fitting the theoretical intensity curve to the experimental by a least-squares refinement. The

procedure is described elsewhere.[20,21] The method is based upon the minimizing of the quantity

$$\sum W \Delta^2$$

where the sum is over all observations. $\Delta = I_{obs} - S \times I_{calc}$, W is the weight of the observation, and S is a scale factor. The program used was essentially as described by Almenningen *et al.*[21] The following weighting scheme was used in the present work:

$$W = \exp[-W_1(s_1 - s)^2] \quad \text{for } s < s_1$$
$$W = 1.00 \quad \text{for } s_1 \leqq s \leqq s_2$$
$$W = \exp[-W_2(s_2 - s)^2] \quad \text{for } s > s_2$$

W_1, W_2, s_1, and s_2 are adjustable constants. In most cases eqn. (7) was used to calculate the theoretical intensity. The program also permits calculation of the intensity according to the more general formula:

$$I(s) = \text{const} \sum_{i \neq j}\sum a_{ij} g_{ij}(s) \exp(-\tfrac{1}{2}u_{ij}^2 s^2) \frac{\sin[(r_{ij} - \varkappa_{ij} s^2)s]}{r_{ij}} \qquad (12)$$

where the following parameters may be refined:

a_{ij}, r_{ij}, u_{ij}, and $\varkappa_{ij}$.

Some of the distances may be treated as dependent parameters according to geometrical restrictions. For the regular octahedral model we thus have only one independent distance parameter if the shrinkage effect is neglected. However, three distances have been treated as independent parameters in the refinements to be described.

Four experimental intensity curves in the range $s = 1.50 - 39.25$ Å^{-1} were obtained by scaling one long distance plate to one of the medium distance plates. The distances and u values were determined from each individual curve by a least-squares refinement. The theoretical intensity was calculated according to eqn. (7) with $g_{ij}(s)$ given by (9), and the f values were as given in the footnote on p. 1958. The results are given in Table 1 a-d. The standard deviations obtained by this procedure are given in parentheses. The mean of these four determinations is given in Table 1 e. The standard deviations in this column are calculated by the usual formula

$$\sigma = [\sum_{i=1}^{n} (\bar{p} - p_i)^2 / (n - 1)]^{\frac{1}{2}}$$

where p_i is an observation of a certain parameter, and $\bar{p}$ is the mean of this parameter. The standard deviation of the *mean value* is thus $\frac{1}{2}(1/\sqrt{n})$ times the value given in column e. In this case $n = 4$, and statistical significance can of course not be claimed. The standard deviations obtained in this way are considerably higher for the UF parameters than the corresponding values given in Table 1 a-d. This is in agreement with the general experience that the standard deviations obtained by the least-squares refinement tend to be too small for accurately determined parameters.[21]

Table 1. Results of least-squares refinements on various intensity curves all ranging from $s = 1.50$ Å^{-1} to $s = 39.25$ Å^{-1}. Standard deviations are given in parentheses. All values in Å.

	a	b	c	d	e	f
r_1	1.999_8 (0.0009)	2.000_3 (0.0008)	1.998_4 (0.0008)	2.002_4 (0.0009)	2.000_2 (0.0017)	2.000_2 (0.0007)
r_2	2.833 (0.0127)	2.829 (0.0114)	2.828 (0.0099)	2.839 (0.0112)	2.832 (0.0050)	2.832 (0.0091)
r_3	4.020 (0.0182)	3.995 (0.0234)	4.005 (0.0137)	3.985 (0.0330)	4.001 (0.0148)	3.999 (0.0181)
u_1	0.046_2 (0.0014)	0.044_3 (0.0014)	0.040_7 (0.0015)	0.044_6 (0.0014)	0.044_0 (0.0023)	0.044_0 (0.0011)
u_2	0.125 (0.0106)	0.119 (0.0096)	0.104 (0.0084)	0.120 (0.0097)	0.117 (0.0091)	0.118 (0.0076)
u_3	0.046 (0.0190)	0.059 (0.0213)	0.028 (0.0202)	0.076 (0.0278)	0.052 (0.0203)	0.056 (0.0167)

In all cases $W_1 = 0.100$, $s_1 = 5.00$ Å^{-1}, $W_2 = 0.006$, $s_2 = 20.00$ Å^{-1}.
a,b,c,d : Individual intensity curves.
e : Mean and standard deviation calculated from the values in Table 1 a,b,c, and d.
f : The mean of the four curves was used as observed intensity data.

The four individual intensity functions were then averaged, and a new least-squares refinement was performed. The results are given in Table 1 f. The standard deviations are of course somewhat smaller than for the individual curves. One might perhaps expect a reduction to approximately one half of the original value. This is, however, not the case. The main reason for this fact is that the value of $\sum W\Delta^2$ is greatly influenced by errors in the background, and even when all the plates are treated separately there are usually similar errors in the backgrounds.

Four of the intensity curves from the plates taken with the shortest camera distance were then averaged and scaled to the mean intensity curve from the other distances. The complete intensity curve ranging from $s = 1.50$ Å^{-1} to 44.25 Å^{-1} was used in the rest of the work. Various least-squares results are shown in Table 2. The results in Table 2 a, b, and c show the effect of changes in the weighting of the data. All the conditions were the same in these refinements except the constant s_2. The f values were the same as before (footnote p. 1958). The parameters in Table 2 b were obtained with the same constants in the weighting scheme as before (Table 1). The constant s_2 was then changed to give more weight to the intensity values at high s values. The results are shown in Table 2c. The difference between the U—F parameters in columns b and c is slightly larger than the corresponding standard deviations, while the F... F parameters are shifted much less than the standard deviations. There is also an increase in the standard deviations of the F... F parameters. This is reasonable since the contribution from these distances are very small at high s values. The results in Table 2 a were obtained with a value of s_2 between the values used in b and c. This weighting scheme is perhaps the most realistic one. The observation at $s = 40$ Å^{-1} is for example given the following weights in the schemes used to obtain the results in a, b, and c: 0.26, 0.09, and 0.86.

The next column (d) shows the refined parameters when scattering amplitudes from Ibers and Hoerni [13] were used. Since these values were calculated for a somewhat shorter electron wave length than was used in this experiment, the corrections suggested by Ibers and Hoerni were applied. This may have introduced some additional uncertainty. Another uncertainty is introduced by the fact that the $|f|$ values for the light atoms are given with too few digits. By comparing the results in Table 2 a and d it is seen that the difference in the estimates of the u value for the U—F distance is rather large, while the shifts in all the other parameters are very small compared to the standard deviations. The standard deviations are higher in column d than in a for all the parameters, indicating that the agreement between the observed and calculated intensities is better when scattering amplitudes according to Karle and Bonham are used.

A refinement based upon the theoretical intensity function including anharmonicity (eqn. (10)), was also performed (Table 2 e). Only the U—F distance was considered anharmonic. The $\varkappa$ value obtained is rather large and depends somewhat on the choice of the constants in the weighting scheme. With the constants used in Table 2 a $\varkappa = 6.2 \times 10^{-6}$ Å^3, and with the constants in Table 2 c $\varkappa = 4.7 \times 10^{-6}$ Å^3. The standard deviation is very large for this parameter. ($\approx 2 \times 10^{-6}$ Å^3). As already mentioned the comparison of the experimental and theoretical RD curves also suggests a large $\varkappa$ value.

Table 2. Results of least-squares refinements on intensity data ranging from $s = 1.50$ Å^{-1} to $s = 44.25$ Å^{-1}. Standard deviations are given in parentheses. All values in Å.

	a	b	c	d	e	f	g
r_1	1.997_7 (0.0006)	1.998_2 (0.0006)	1.997_5 (0.0006)	1.997_7 (0.0008)	2.002_0 (0.0016)	1.997_8 (0.0006)	
r_2	2.833 (0.0092)	2.833 (0.0084)	2.833 (0.0099)	2.831 (0.0113)	2.833 (0.0090)	2.830 (0.0084)	
r_3	3.994 (0.0189)	3.992 (0.0168)	3.994 (0.0219)	3.994 (0.0248)	3.994 (0.0185)	3.995 (0.0176)	
u_1	0.044_8 (0.0009)	0.044_2 (0.0010)	0.045_4 (0.0008)	0.040_7 (0.0012)	0.044_9 (0.0009)	0.043_0 (0.0009)	0.0425
u_2	0.121 (0.0076)	0.121 (0.0070)	0.122 (0.0082)	0.116 (0.0093)	0.122 (0.0075)	0.118 (0.0093)	0.1215
u_3	0.062 (0.0161)	0.058 (0.0153)	0.066 (0.0179)	0.060 (0.0206)	0.062 (0.0158)	0.060 (0.0155)	0.0595

a: Constants in the weighting scheme: $W_1 = 0.100$, $s_1 = 5.00$ Å^{-1}, $W_2 = 0.006$, $s_2 = 25.00$ Å^{-1}. f values from Karle and Bonham (footnote p. 1958). The theoretical intensity was calculated in the harmonic approximation (eqn. (7)).

b: $s_2 = 20.00$ Å^{-1} All other conditions as in a.

c: $s_2 = 35.00$ Å^{-1} » » » » » »

d: f values from Ibers and Hoerni. » » » » » »

e: The theoretical intensity was calculated from eqn. (10). (Anharmonic). All other conditions as in a. The refinement gave $\varkappa_{UF} = 6.2 \times 10^{-6}$ Å^3 with a standard deviation of 2.2×10^{-6} Å^3. (With $s_2 = 35.00$ Å^{-1} as in c the result was $\varkappa_{UF} = 4.7 \times 10^{-6}$ Å^3 (1.8×10^{-6} Å^3)).

f: The experimental $g_{UF}(s)$ function (Fig. 6) was used. The scale of this curve was refined in addition to r and u values. All other conditions as in a.

g: Spectroscopic values from Cyvin *et al.*

Using the formula suggested by Bartell [6,7]

$$\varkappa = au^4/6$$

we obtain $a = 9.2$ Å^{-1} and $a = 7.0$ Å^{-1} with the $\varkappa$ values given above. Usually a is 2.0 — 3.0 Å^{-1}.

It is worth mentioning that the parameter α_{UF} in eqn. (12) was also refined. ($\varkappa_{UF}$ was then kept equal to zero). The result was $\alpha_{UF} = 1.077$ with a standard deviation of 0.095. The distance- and u parameters were almost identical to the values in Table 2 a. In agreement with this least-squares result it is observed that the area of the U—F double peak is larger, compared to the F...F peaks, on the experimental RD curve than on the theoretical one (Fig. 1). The experimental result is, however, very uncertain as the standard deviation of α_{UF} shows.

The distances found by the least-squares procedure correspond closely to the distances denoted by $r_g(1)$.[6] We have

$$r_g = r_g(1) + u^2/r \qquad (13)$$

Table 3 a shows the r_g distances calculated using the results in Table 2 a.

Table 3. Comparison of the non-bonded distances in UF_6 obtained as independent parameters in the least-squares refinement, and values calculated from the bond length assuming O_h symmetry.

	a	b	c	d
U—F	1.998$_7$			
F. . .F (1)	2.838	2.827	0.002	2.825
F. . .F (2)	3.996	3.996	0.009	3.987

a: r_g distances calculated by eqn. (13) and values from Table 2 a.
b: Non-bonded distances calculated from the bond length assuming a rigid molecule.
c: Shrinkage calculated by Cyvin *et al.*
d: Values in (b) — values in (c).

Assuming a rigid octahedral molecule, the F... F values in Table 3 b follow from the bond length. However, the shrinkage should be subtracted from these values before a comparison with Table 3 a is made. The shrinkage calculated by Cyvin *et al.*[22] is given in column c, and the corrected distances are given in column d. We observe that both distances are somewhat shorter than given in Table 3 a. The difference is slightly greater than the standard deviation for the short F...F distance, but it is doubtful whether the difference is significant. The contribution from this distance to the molecular intensity falls off rapidly with s because of the large u value. Effects neglected in the scattering theory used (*i.e.* polarization [23]), are largest for small s values. It is hoped that most of the defects are eliminated by drawing an experimental background, but there may be effects not completely compensated in this manner. Further, it is usually difficult to draw the experimental background for small s values.

The minimum of the U—F double peak in the RD curve is at 1.998 Å and the maximum of the first F ... F peak at 2.823 Å. By adding u^2/r to these values we obtain 1.999 Å and 2.828 Å in better agreement with the geometrical restriction.

We may conclude that there is no significant deviation from O_h symmetry. The bond length is 1.999 Å (r_g) with an estimated standard deviation of 0.003 Å. This standard deviation includes systematic errors; the most important of these is the uncertainty in the wave length. [5]

SCATTERING AMPLITUDES

The results given in Table 2 a and d were obtained using scattering amplitudes calculated by different authors. The function

$$g_{UF}(s) = \frac{|f_U|}{|f_F|} \cos(\eta_U - \eta_F) \quad (14)$$

calculated using values for $|f|$ and η according to Karle and Bonham, is shown as the dashed curve in Fig. 4 a. Fig. 4 b (dashed curve) shows the same function calculated with values from Ibers and Hoerni. It should be observed that the first zero point is at a slightly higher s value in Fig. 4 b. The difference between the two sets of scattering amplitudes is probably due mainly to the use of different scattering potentials. The refined parameters in Table 2 a and d confirm that distance parameters are insensitive to small changes in the scattering amplitudes. (This should at least hold true for distances that give well separated peaks in the RD curve.) However, the u values are rather sensitive to changes in the scattering amplitudes. It is therefore of interest to compare the u values found by electron diffraction to the results obtained by spectroscopic methods. In Table 2 g u values calculated by Cyvin *et al.*[22] (for 25°C) are given. The agreement is satisfactory; the spectroscopic u value for the bond distance being between the corresponding values in Table 2 a and d. This indicates that the scattering amplitudes used are reasonably accurate.

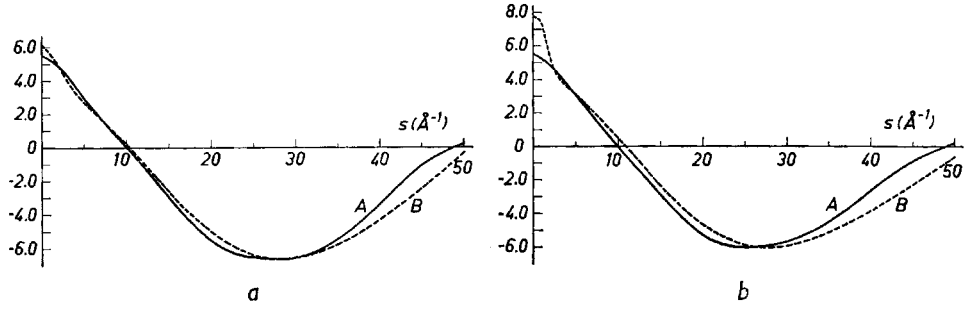

Fig. 4 a,b. An experimental curve (A) for the function $g_{UF}(s)$ (eqn. (14)) compared to theoretical curve B (dashed). Theoretical values according to a. Karle and Bonham.[16] b. Ibers and Hoerni.[13]

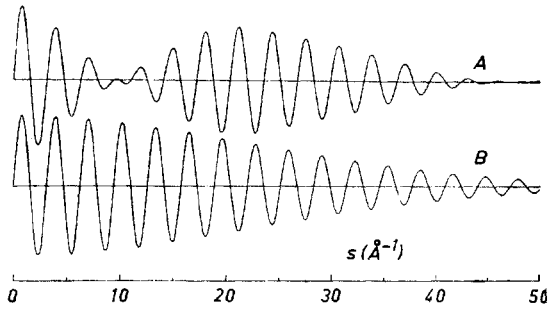

Fig. 5. Curve A was obtained by a Fourier transformation of curve A in Fig. 3 and gives the U—F contribution to the intensity. Curve B shows the damped sine curve [const. × $\exp(-\frac{1}{2}u_1^2s^2)$ sin (r_1s)] with u_1 and r_1 as given in Table 2 a.

It is possible to demonstrate in a very simple way how the theoretical scattering amplitudes fit the experimental date. Fig. 5 (curve A) shows the contribution from the U—F bonds to the experimental intensity. This curve was obtained by a Fourier transformation of the experimental RD curve in Fig. 3 (curve A). One could, of course, subtract the F... F contribution from the total intensity. However, the Fourier transformations have the advantage of eliminating some random errors. The procedure depends upon a proper drawing of the envelope (zero-line) in the experimental RD curve. Reasonably different envelopes were tried giving very similar U—F intensity curves; only the inner peak changed significantly. Because of noise it is difficult to know exactly how the double peak falls off towards zero. A U—F intensity curve similar to the one in Fig. 5, was calculated by smoothing out the noise in the experimental RD curve (Fig. 3, curve A) before the Fourier transformation. The intensity curves differed significantly only for $s > 41$ Å^{-1}. The function

$$\text{const.} \times \exp(-\tfrac{1}{2}u_1^2s^2) \sin(r_1s) \qquad (15)$$

is also shown in Fig. 5 (curve B). The values for r_1 and u_1 are given in Table 2 a. By dividing an experimental U—F intensity curve by this damped sine curve, experimental values for the function $g_{UF}(s)$ (eqn. (14)) are obtained. It is, of course, not possible to use values near a zero point in the damped sine curve. Instead three points around the maxima and minima were used. The crosses in Fig. 6 show the experimental results when curve A in Fig. 5 was used for the experimental U—F intensity. The circles were obtained with the other experimental U—F intensity obtained as described above. The curve is drawn through the experimental points. This curve is compared to the theoretical $g_{UF}(s)$ function (dashed curve) calculated according to Karle and Bonham in Fig. 4a. The experimental curve was scaled to give the two functions the same minimum value.

A damped sine curve was then calculated according to eqn. (15) using the values in Table 2 d for r_1 and u_1. An experimental $g_{UF}(s)$ function was obtained in the same way as before. This curve is compared to the theoretical function calculated using scattering amplitudes from Ibers and Hoerni, in Fig. 4 b.

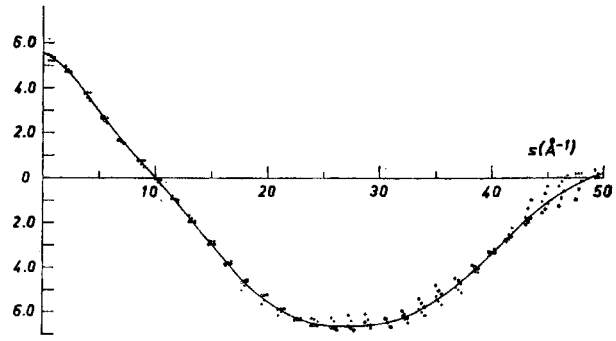

Fig. 6. Experimental values for the function $g_{UF}(s)$ obtained by dividing an experimental U—F intensity function by the damped sine curve in Fig. 5. The points marked with + were obtained with the experimental U—F intensity curve in Fig. 5, and the points marked with O give the values obtained with the other experimental U—F curve. (See text). The curve is drawn through the experimental points.

The agreement between the experimental and theoretical curves is somewhat better in Fig. 4 a than in Fig. 4 b, though the agreement is reasonably good also in the latter case. The experimental values should be well determined in the region close to the first zero point. This zero point is at $s = 10.0$ Å^{-1} on the experimental curves compared to $s = 10.36$ Å^{-1} on the theoretical curve in Fig. 4 a, and $s = 10.89$ Å^{-1} on the theoretical curve in Fig. 4 b. The second zero point is at $s \approx 49$ Å^{-1} on the experimental curves compared to $s = 50.8$ Å^{-1} and $s = 52.0$ Å^{-1} on the theoretical curves. The experimental points are, however, very uncertain in this region.

The experimental curve in Fig. 6 was now used in a least-squares refinement of distances and u values. The scale (a_{UF} in eqn. (12)) of the experimental $g_{UF}(s)$ function was refined at the same time. The results are given in Table 2 f. As to be expected the distance parameters are very close to the values in Table 2 a. Only the shift in the u value for the U—F distance is greater than

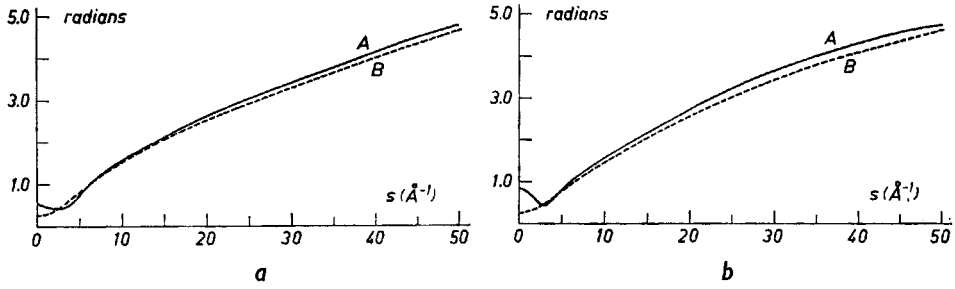

Fig. 7a, b. $\Delta\eta_{UF}(s)$ obtained from the experimental $g_{UF}(s)$ functions in Fig. 4 and theoretical $|f|$ values (A) compared to theoretical $\Delta\eta_{UF}(s)$ functions (B). a. Experimental $g_{UF}(s)$ function from Fig. 4 a and theoretical $|f|$ values from Karle and Bonham.[15] b. Experimental $g_{UF}(s)$ function from Fig. 4 b and theoretical $|f|$ values from Ibers and Hoerni.[18]

the corresponding standard deviation, the result now being very close to the value found by Cyvin *et al.* [22] (Table 2 g).

It proved difficult to find experimental values for all the functions $|f_U|$, $|f_F|$, $\Delta\eta_{UF}$ included in the function $g_{UF}(s)$ (eqn. (14)). Since the shape of the function $|f_U|/|f_F|$ seems to be rather insensitive to the calculation method used (including even the first Born approximation), it is of interest to divide the experimental $g_{UF}(s)$ function by the corresponding theoretical $|f_U|/|f_F|$ function. In this way functions for $\Delta\eta_{UF}(s)$ based upon the experimental data and theoretical $|f|$ values are found. These curves are compared to the theoretical functions (dashed curves) in Fig. 7 a and b. As before the agreement is somewhat better for scattering amplitudes according to Karle and Bonham (Fig. 7 a) than for values from Ibers and Hoerni (Fig. 7 b).

Acknowledgement. The author is grateful to the members of the Electron Diffraction Group in Oslo, especially Professor O. Bastiansen for helpful discussions, Dr. A. Haaland for taking the diffraction photographs, and Miss Snefrid Gullikstad for doing much of the calculations. Thanks are also due to Professor R. A. Bonham, Lic. techn. T. Strand and Indiana University Research Computing Center for the calculation of the necessary scattering amplitudes.

REFERENCES

1. Merzbacher, E. *Quantum Mechanics*, Wiley, New York 1961.
2. Shiff, L.I. *Quantum Mechanics*, 2nd Ed., McGraw Hill, New York 1955.
3. Mott, N.F. and Massey, H.S.W. *The Theory of Atomic Collisions*, Oxford University Press, London 1949.
4. Spiridonov, V.P., Rambidi, N.G. and Alekseev, N.V. *Zh. Strukt. Khim.* **4** (1963) 779; *J. Struct Chem. (USSR)* **4** (1963) 717.
5. Almenningen, A., Bastiansen, O., Haaland, A. and Seip, H.M. *Angew. Chem.* **77** (1965) 877.
6. Bartell, L.S. *J. Chem. Phys.* **23** (1955) 1219.
7. Kuchitsu, K. and Bartell, L.S. *J. Chem. Phys.* **35** (1961) 1945.
8. Broune, H. and Pennow, P. *Z. physik. Chem.* **B 35** (1937) 239.
9. Bauer, S.H. *J. Chem. Phys.* **18** (1950) 27.
10. Gaunt, J. *Trans. Faraday Soc.* **49** (1953) 1122.
11. Schomaker, V. and Glauber, R. *Nature* **170** (1952) 290.
12. Glauber, R. and Schomaker, V. *Phys. Rev.* **89** (1953) 667.
13. Ibers, J.A. and Hoerni, J.A. *Acta Cryst.* **7** (1954) 405.
14. Bonham, R.A. and Karle, J. *J. Phys. Soc. Japan.* **17** *Suppl.* **B—II** (1962) 6.
15. Karle, J. and Bonham, R.A. *J. Chem. Phys.* **40** (1964) 1396.
16. Schomaker, V., Glauber, R., Bastiansen, O., Scheehan, W.F., Felsenfeld, G. and Ibers, J. *Chem. and Chem. Eng. Calif. Inst. Techn.* 1951—1952, 7.
17. Hoerni, J.A. and Ibers, J.A. *Phys. Rev.* **91** (1953) 1182.
18. Bastiansen, O. and Skancke, P. N. *Advan. Chem. Phys.* **3** (1960) 323.
19. Hanson, H.P., Herman, F., Lea, J.D. and Skillman, S. *Acta Cryst.* **17** (1964) 1040.
20. Hedberg, K. and Iwasaki, M. *Acta Cryst.* **17** (1964) 529.
21. Almenningen, A., Bastiansen, O., Seip, R. and Seip, H.M. *Acta Chem. Scand.* **18** (1964) 2115.
22. Meisingseth, E., Brunvoll, J. and Cyvin, S.J. *Kgl. Norske Videnskab. Selskabs, Skrifter* **1964** No. 7.
23. Bonham, R.A. *J. Chem. Phys.* **43** (1965) 1933.

Received July 2, 1965.